01-11940

THE EFFECT OF DIFFUSION ON THE DEACTIVATION OF CATALYSTS
USED FOR HYDROCRACKING ATHABASCA BITUMEN

M.A. Altajam, J.F. Kriz, and M. Ternan
Synthetic Fuels Research Laboratory

October 1990

ERL 90-60 (J)

THE EFFECT OF DIFFUSION ON THE DEACTIVATION OF CATALYSTS USED FOR HYDROCRACKING ATHABASCA BITUMEN

M.A. ALTAJAM[1], J.F. KRIZ, and M. TERNAN

Energy Research Laboratories / CANMET, Energy, Mines and Resources Canada, Ottawa, Ontario, K1A 0G1, Canada

ABSTRACT

The deactivation of alumina supported and carbon supported Co-Mo catalysts was studied while hydrocracking Athabasca bitumen. Diffusion rates were different because the pore diameters were different in alumina and carbon catalysts. Diffusion rates also changed because the length of the diffusion path in the alumina catalyst was altered by using 3.2 and 1.6 mm diameter extrudates as well as powdered catalyst.

INTRODUCTION

The commercial Co-Mo catalysts used for hydrocracking oil sands bitumen and petroleum residua are normally supported on alumina. Several years ago hydrodesulphurization (HDS) studies with thiophene (ref. 1) indicated that carbon supported catalysts were superior to alumina supported ones. However HDS of benzothiophene (ref. 2) was found to be greater on alumina supported catalysts than on carbon supported ones. Studies of these two supports were performed in our laboratory with Athabasca bitumen (ref. 3). Care was required in choosing the particular carbon support, since carbons which have very large surface areas also have small pore sizes which would inhibit or perhaps exclude some of the larger molecular species in resid feedstocks, such as Athabasca bitumen. The wide pore carbon that was available, had a surface area and a median pore diameter that were respectively half and more than double those of the alumina support used for comparison. The results of our study (ref. 3) showed that HDS conversions were better with the large surface area alumina catalyst. However, when the results were compared on the basis of a unit of catalyst surface area, the carbon supported catalyst was superior. The present investigation of deactivation is an extension of the earlier work (ref. 3). Although the results can be expressed on the basis of unit surface area, because the pore diameters are different, the contribution of diffusion to deactivation was also expected to be different.

Deactivation measurements were made using three catalysts. The two alumina catalysts were identical except that their extrudate diameters were 3.2 and 1.6 mm respectively, and thereby provided different diffusion path lengths. Descriptions of the catalysts and the bitumen (ref. 3) from which this vacuum resid was obtained plus the equipment (ref. 4) have been reported. Some catalyst properties are in Table 1.

TABLE 1
Catalyst properties

Support	Al_2O_3	Carbon
MoO$_3$ wt %	15.0	15.0
CoO wt %	3.0	3.0
Bulk density g/mL	0.74-0.78	0.438
Surface Area m^2/g	210	116
Median Pore Dia nm	8.5	28.6

TABLE 2
Rate constants from Equation 7

	k_D x 10^3 (s^{-1})			k_S x 10^5 (s^{-1})		
Cat	Alumina		C	Alumina		C
Dia mm	3.2	1.6		3.2	1.6	
HDS	6.8	5.6	13.8	10.3	11.0	5.0
HDAsp	12.7	11.6	16.8	7.4	8.1	5.2
HDV	9.4	7.9	14.5	6.9	7.3	6.2
HDNi	9.4	7.4	3.2	9.6	10.0	9.6
MCR/A	12.8	10.1	21.9			
+525/A	5.0	4.3	5.2			

The hydrocracking reaction conditions were 13.9 MPa, 425°C, liquid space velocity 0.67 h^{-1}, and hydrogen rate 10 L H$_2$(STP)/L oil.
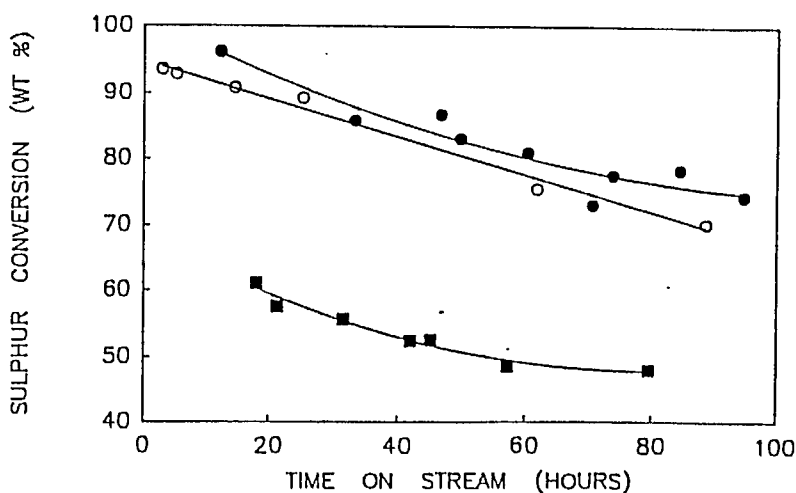

Figure 1 Sulphur Conversion (wt %) Versus Time on Stream (hours) - open circles, solid circles, and solid squares represent the 3.2 mm and the 1.6 mm alumina supported catalysts, and the carbon supported catalysts respectively.

RESULTS AND DISCUSSION

Hydrodesulphurization (HDS) is shown in Figure 1 as a function of time on stream. All of the catalysts deactivated continuously. The carbon supported catalyst produced much lower conversions than the alumina supported catalysts, which is consistent with our previous work (ref. 3) and was probably caused by the smaller surface area of the carbon supported catalyst (Table 1).

The Turnover Frequency (TOF) is often defined as the number of molecules reacting per second per site on the catalyst. Since the number of reaction sites on the catalysts was not known, the Pseudo Turnover Frequency (PTOF), the number of reactions per unit time per unit surface area, PTOF, was used in Figures 2 to 7.

Some of the conversion occurred on the catalyst surface and some occurred by thermal reactions in the void spaces between the catalyst particles. An experiment with stainless steel balls in the reactor was performed to simulate the reactor volume available for thermal reactions. This thermal conversion was subtracted from the conversion obtained in the presence of the catalysts (catalytic plus thermal) in order to obtain a conversion, X_{CAT}, that could be attributed to the catalyst alone. This was the conversion used to calculate the PTOF using Equation 1.

$$PTOF = (C_R \ X_{CAT}) / (\rho_{CAT} \ A \ \theta_R) \tag{1}$$

where A is the total surface area in the reactor, C_R is the concentration of the reactant in the feedstock, ρ_{CAT} is the bulk density of the catalyst in the reactor, and θ_R is the residence time in the reactor.

Figures 2 to 7 show PTOF's for the following reactions: HDS, hydrodeasphalting (HDA), hydrodemetallization (HDM), specifically hydrodevanadization (HDV) and hydrodenickelization (HDNi), microcarbon residue conversion divided by total surface area in the reactor (MCR/A), and $+525^{O}C$ conversion divided by total surface area (+525/A). The MCR content of reaction product samples was used to calculate the fraction of $+525^{O}C$ material in the sample, using a correlation (ref. 5). Asphaltenes were measured by insolubility in n-pentane.

The deactivation shown in the above figures can be described quantitatively, by assuming that the rate of deactivation is first order in the number of reaction sites per unit of catalyst surface area, C^*
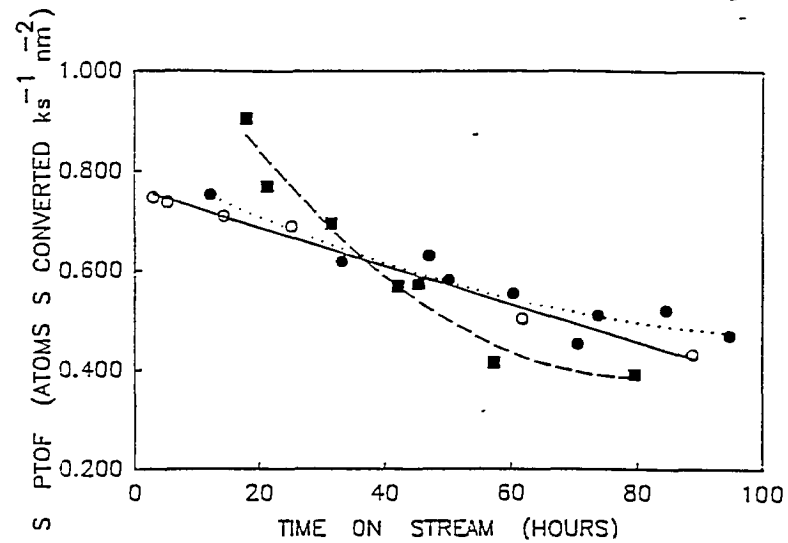
$$- dC^* / d\theta_{TOS} = k_D \ C^* \tag{2}$$

Figure 2 Sulphur Pseudo Turnover Frequency (atoms S converted ks^{-1} nm^{-2}) Versus Time on Stream (hours) – open circles (solid line), solid circles (dotted line), and solid squares (dashed line) represent the 3.2 mm, the 1.6 mm alumina supported catalysts, and the carbon supported cataysts respectively
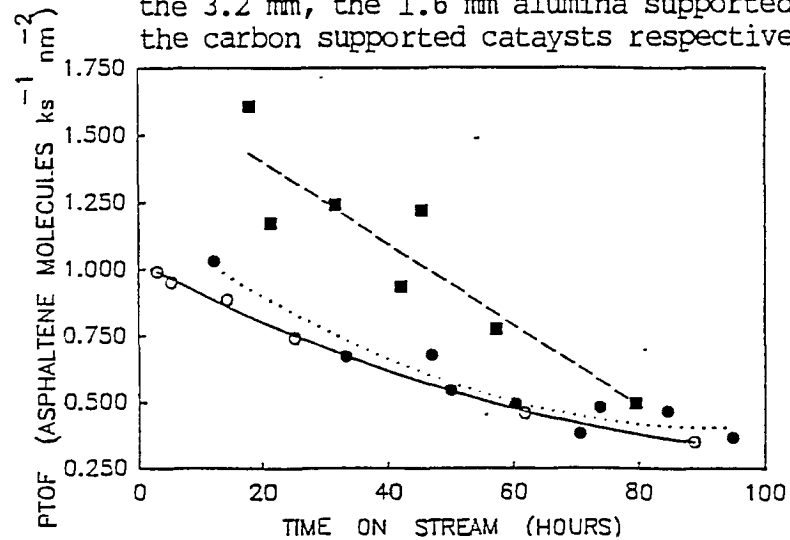

Figure 3 Asphaltene Pseudo Turnover Frequency (asphaltene molecules ks^{-1} nm^{-2}) Versus Time on Stream (hours) – symbols as given in Figure 2
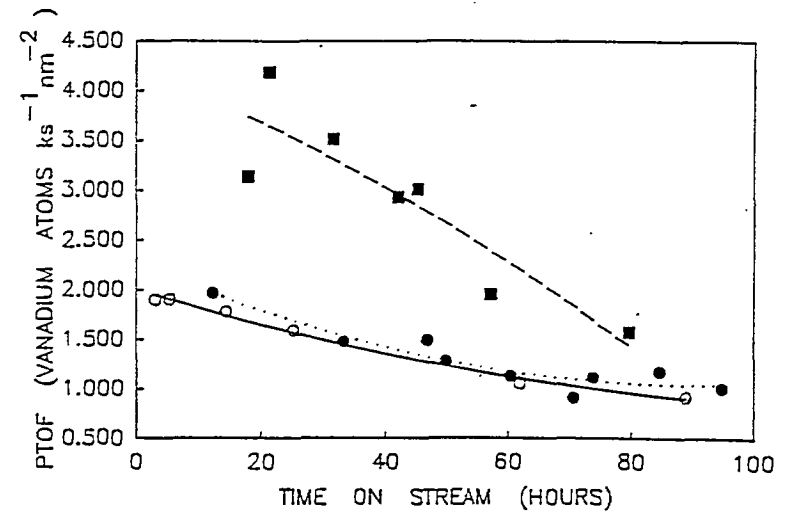

Figure 4 Vanadium Removal Pseudo Turnover Frequency (atoms V ks^{-1} nm^{-2}) Versus Time on Stream (hours) – symbols as given in Figure 2
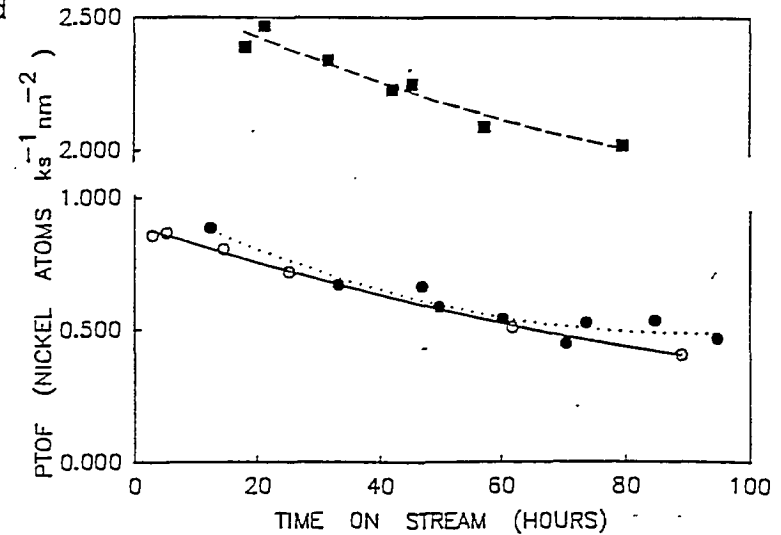

Figure 5 Nickel Removal Pseudo Turnover Frequency (atoms Ni removed ks^{-1} nm^{-2}) Versus Time on Stream (hours) – symbols as given in Figure 2

where k_D is the first order deactivation constant and θ_{TOS} is the time on stream. Equation 2 can be integrated to obtain

$$c^* = c_o^* \exp(-k_D\theta_{TOS}) \tag{3}$$

where c_o^* is the initial surface concentration of reaction sites on the catalyst, prior to deactivation.

The reaction rate of the adsorbed reactant on the catalyst surface can also be written as a first order equation

$$-dC_s / d\theta_R = k_s C_s \tag{4}$$

where C_s is the concentration of adsorbed reactant on the catalyst surface, k_s is the rate constant for the surface reaction, and θ_R is the residence time in the reactor. If all the reaction sites are occupied by an adsorbed reactant molecule, C_s will be equal to c^*, and Equation 3 can be substituted for the value of C_s on the right hand side of Equation 4, but not on the left hand side. Equation 4 can be integrated and expressed in terms of the catalytic conversion, X_{CAT}, (calculated by subtracting the thermal conversion from the conversion obtained with a catalyst).

$$X_{CAT} = k_s\theta_R\exp(-k_D\theta_{TOS}) \tag{5}$$

X_{CAT} from Equation 5 can be substitued into Equation 1 and logarithms taken to obtain

$$\ln PTOF = -k_D\theta_{TOS} + \ln[(k_s C_R) / (\rho_{CAT} A)] \tag{6}$$

The data in Figures 2 to 7 were fitted using Equation 6 to obtain the results for the deactivation rate constant k_D and the surface reaction rate constant k_s shown in Table 2. The correlation coefficients were 0.99 or better for the 3.2 mm extrudates, 0.88 – 0.93 for the 1.6 mm extrudates, and 0.92 – 0.99 for the carbon supported catalysts. These values indicate that Equation 6 provides an acceptable correlation of the deactivation data. The k_s values for the HDS and HDA reactions have the same order of magnitude as those reported in earlier work (ref. 3). In general, the deactivation rate constants are similar for the two alumina supported catalysts. Except for HDNi, all the deactivation rate constants for the carbon supported catalyst are greater than those for the alumina supported ones.
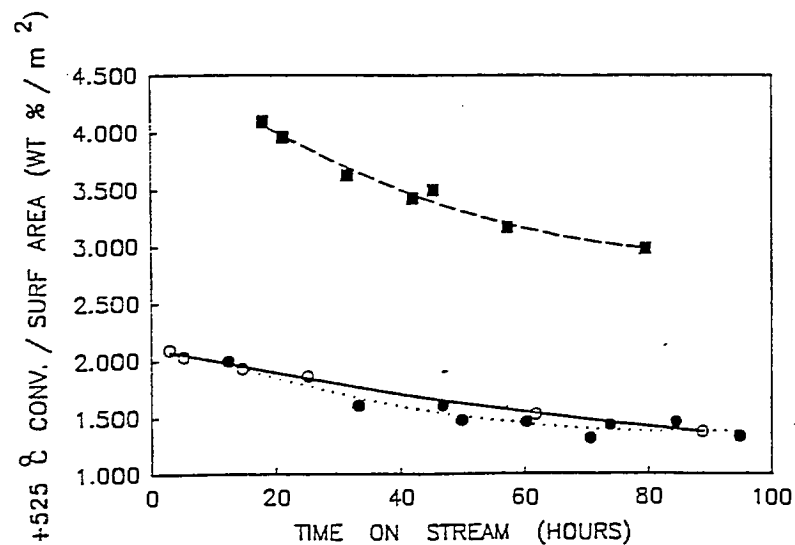
Figure 6 Microcarbon Residue Conversion per Unit of Catalyst Surface Area in the Reactor (wt%/m) x 10^3 Versus Time on Stream (hours) — symbols as given in Figure 2
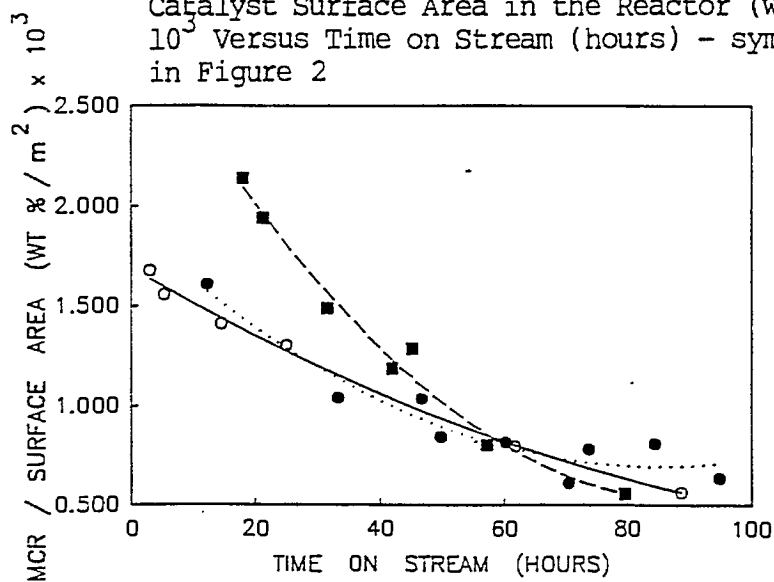

Figure 7 Conversion of the +525°C Fraction per Unit of Catalyst Surface Area in the Reactor (wt %/m^2 x 10^3 Versus Time on Stream (hours) — symbols as given in Figure 2
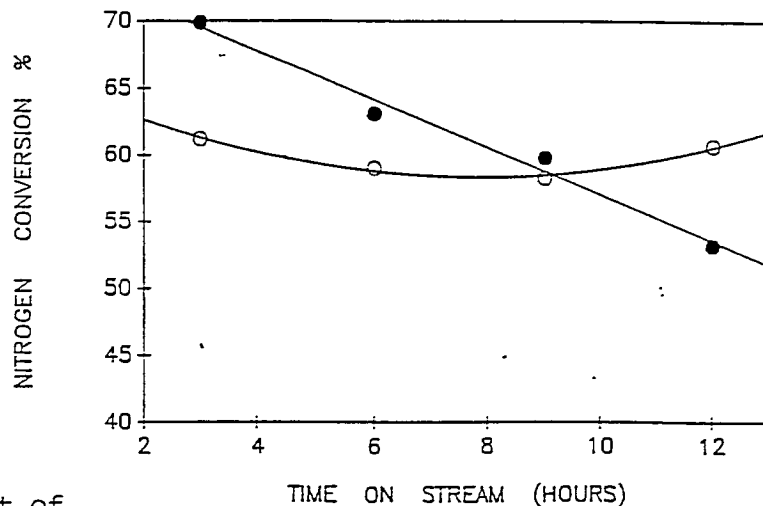

Figure 8 Nitrogen Conversion (wt %) Versus Time on Stream (hours) — open and closed circles are for 3.2 mm extrudates and 0.6 mm powder particles. Both catalysts were Ni-Mo on alumina promoted with F.
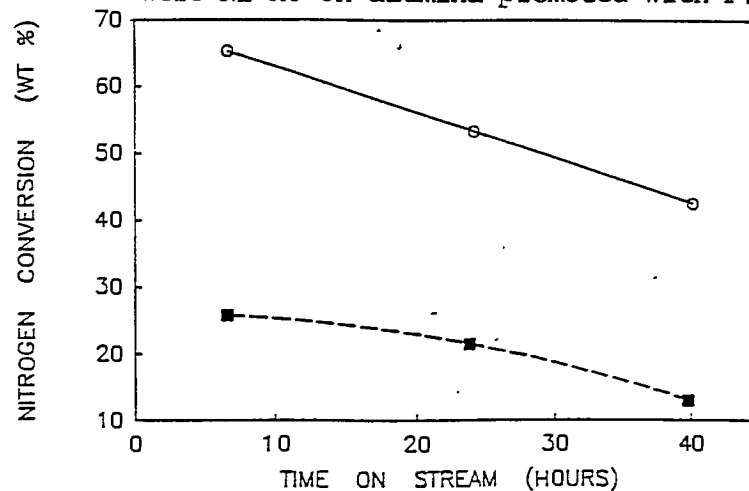

Figure 9. Nitrogen Conversion (wt %) Versus Time on Stream (hours) — open circles represent 3.2 mm extrudates of Co-Mo on alumina, solid squares represent Co-Mo supported on carbon.

Pore diffusion effects can be considered in terms of a theoretical equation (ref. 6) which has been shown to describe the diffusion of petroleum asphaltene molecules,

$$D_{eff} \, / \, D_B \; = \; (1 - \lambda)^2 \, / \, (1 + \lambda P) \qquad\qquad (7)$$

where D_{eff} is the effective diffusivity of the liquid phase molecule in the pore, D_B is its diffusivity in the bulk liquid, λ is equal to d_m/d_p, (d_m is the diameter of the diffusing molecule and d_p is the pore diameter), and P is a parameter which sums a number of terms that were used in the original derivation of Equation 7 (ref. 6).

Equation 8, which was obtained from Equation 7, shows the ratio of effective diffusivities for the carbon and alumina catalysts.

$$(D_{eff})_C \, / \, (D_{eff})_{Al} \; = \; (1 - \lambda)^2_C \, / \, (1 - \lambda)^2_{Al} \qquad\qquad (8)$$

λ values for the alumina and carbon catalysts in Equation 8 were calculated by assuming that a typical molecule has a molecular diameter of 2 nm. On this basis, it was calculated that the effective diffusivity should be 1.5 times greater in the carbon catalyst than in the alumina catalysts. For the reactions that do not deactivate as quickly on the carbon catalyst, HDNi and +525/A, the PTOF's were more than 1.5 times greater. This suggests that although diffusion affects conversion it does not totally "control" conversion.

A comparison of the two different alumina catalysts in Figures 2 to 7 shows the differences in PTOF's caused by differences in diffusion path length. The smaller diameter extrudates had a slightly greater PTOF's but the k_D's were similar. In Figure 8 the difference in diffusion path length was more pronounced. A 3.2 mm extruded Ni-Mo/Al$_2$O$_3$ catalyst, promoted with fluoride ions, was compared with the same catalyst in the form of powder having typical diameters of 0.6 mm. It can be seen that the hydrodenitrogenation (HDN), shown as nitrogen conversion, decreases for the powder but not for the 3.2 mm extrudates. Similar results have also been reported for Ni-Mo/Al$_2$O$_3$ catalysts that were promoted with both Li and F ions (ref. 7). It has been shown (ref. 8) that the shorter diffusion path length causes the concentration of the adsorbing species to be much greater in the interior of the small catalyst particles. These concentrations cause greater reaction rates, which cause greater deactivation by metals deposition. Interestingly, the HDS deactivation was similar for both the small particle catalyst and the extruded catalyst (ref. 7-8).

Figure 9 shows rapid HDN deactivation of Co-Mo catalysts on both alumina and on carbon. The expectation that the carbon catalyst would deactivate quickly because it has a larger median pore diameter was observed. However, deactivation of the Co-Mo on alumina catalyst in Figure 9 was much faster than the Ni-Mo on alumina catalyst in Figure 8. An explanation for these differences may involve both the chemical composition of the catalyst surface as well as the diffusion path length.

CONCLUSIONS

1. Carbon catalysts had greater PTOF's, which caused more metals to be deposited per unit area of catalyst surface, and resulted in greater deactivation for most reactions.

2. For the carbon supported catalyst, the HDNi and +525/A deactivations were not as rapid as the other reactions.

3. Ni-Mo and Co-Mo on alumina catalysts have different HDN deactivation.

REFERENCES
1. G.C. Stevens and T. Edmonds, Preparation and properties of thiomolybdate graphite catalysts, in Preparation of catalysts II (eds. B. Delmon, P. Grange, P. Jacobs, and G. Poncelet), Elsevier, Amsterdam, 1979, pp. 507-517.
2. F.P. Daly, J.S. Brinen, and J.L. Schmitt, A wide pore carbon supported hydrodesulphurization catalyst, Appl. Catal. 11 (1984) 161-164.
3. M.A. Altajam and M. Ternan, Hydrocracking of Athabasca bitumen using Co-Mo catalysts supported on wide pore carbon extrudates, Fuel, 68 (1989) 955-960.
4. M. Ternan, Catalytic hydrogenation and asphaltene conversion of Athabasca bitumen, Can. J. Chem. Eng. 61 (1983) 689-696.
5. M. Ternan and J.F. Kriz, +525°C pitch content versus microcarbon residue: A correlation for characterizing reaction products obtained by hydrocracking bitumens, heavy oils, and petroleum residue, AOSTRA J. Res., 6 (1990) 65-70.
6. M. Ternan, The diffusion of liquids in pores, Can. J. Chem. Eng., 65 (1987) 244-249.
7. J.F. Kriz, J. Monnier, and M. Ternan, Nickel - molybdenum - alumina catalysts: Effects of doping with fluoride and lithium and changes in particulate size when applied to bitumen hydroprocessing, Preprints, 11th Can. Symp. Catal. 11 (1990) 201-210.

8. J.F. Kriz, J. Monnier, and M. Ternan, Bitumen hydroprocessing: Nickel - molybdenum - alumina catalysts doped with fluoride and/or lithium, AIChE Symp. Ser., Tar Sand and Oil Upgrading, (eds. S.S. Shih and C.M. Oballa) (submitted for publication).